Journal of Materials Chemistry B

ROYAL SOCIETY OF CHEMISTRY

REVIEW

View Article Online
View Journal | View Issue

Cite this: J. Mater. Chem. B, 2020, 8, 863

Beyond Fmoc: a review of aromatic peptide capping groups

Adam D. Martin *[a] and Pall Thordarson *[b]

Received 10th November 2019,
Accepted 8th January 2020

DOI: 10.1039/c9tb02539a

rsc.li/materials-b

Self-assembling short peptides have attracted widespread interest due to their tuneable, biocompatible nature and have potential applications in energy materials, tissue engineering, sensing and drug delivery. The hierarchical self-assembly of these peptides is highly dependent on the selection of not only amino acid sequence, but also the capping group which is often employed at the N-terminus of the peptide to drive self-assembly. Although the Fmoc (9*H*-fluorenylmethyloxycarbonyl) group is commonly used due to its utility in solid phase peptide synthesis, many other aromatic capping groups have been reported which yield functional, responsive materials. This review explores recent developments in the utilisation of functional, aromatic capping groups beyond the Fmoc group for the creation of redox-responsive, fluorescent and drug delivering hydrogel scaffolds.

Introduction

Self-assembly is a phenomenon which is ubiquitous in nature, from the complementarity of DNA base pairs,[1] to the transport of ions across membranes,[2,3] the folding of proteins into functional tertiary structures,[4,5] self-assembly underlies many of the most fundamental biological processes. The self-assembly of proteins is of particular interest, as the structure of the protein is intricately linked with its function. Two well-known examples of this are observed in Alzheimer's disease, where minor modifications to the amyloid and tau proteins result in the self-assembly and the apparent pathological accumulation of these proteins, resulting in a gain of toxic function.[6,7]

Originally identified as an aggregation-prone region of the amyloid protein, the diphenylalanine sequence has been used in a number of applications, from semi-conductors to nanophotonics, to optics, with excellent reviews available on these topics.[8–10] Perhaps one of the most popular applications of the diphenylalanine motif has been its incorporation into short hydrogel-forming peptides. These hydrogels can be engineered to mimic the physical and mechanical properties of the extracellular matrix and have been extensively reviewed.[11–15]

Often, these diphenylalanine containing, self-assembling peptide hydrogels are "capped" at their N-terminus with an aromatic group. The choice of this capping group plays a key role in the subsequent self-assembly of the peptide. It is known that the diphenylalanine sequence alone (*i.e.*, NH_2-Phe-Phe-OH) will not form hydrogels, instead they tend to form crystalline nanotubes which have excelled in a number of applications.[16–18] The introduction of the fluorenylmethyloxycarbonyl (Fmoc) group to the N-terminus of the diphenylalanine sequence (Fmoc-FF), as first reported by Gazit,[19] resulted in the formation of a self-supporting hydrogel, formed through the dilution of Fmoc-FF dissolved in hexafluoroisopropanol with water. Since this initial study, extensive research effort has been applied to elucidating different ways to initiate gelation,[20,21] minimizing the variability in resultant hydrogel networks (which are gelation-method dependent),[22] and developing applications for these nanostructured scaffolds in tissue engineering, electronics and drug delivery.[23–27]

One reason for the popularity of Fmoc-FF in various applications is its ease of synthesis. Fmoc-FF can be synthesised either using solution or solid phase peptide synthesis methods, owing to the common use of the Fmoc group as an amine protecting group in solid phase peptide synthesis (SPPS) and is also commercially available through Bachem. However, this also means that the Fmoc group is susceptible to cleavage at pH values above 10, which can be problematic, as Fmoc-containing peptide gelators are often dissolved in basic aqueous solutions prior to initialising gelation. Upon cleavage of the Fmoc-group from a peptide chain, a highly reactive dibenzofulvalene is formed. While the toxicity of dibenzofulvalene coming from Fmoc-based peptides has not been determined directly, our studies have indicated that Fmoc-FF degradation products show some cytotoxicity.[28]

In order to bypass this, a number of different capping groups have been used. The Adams group have popularised the use of a

[a] Dementia Research Centre, Department of Biomedical Science, Faculty of Medicine and Health Sciences, Macquarie University, Sydney, NSW 2109, Australia. E-mail: adam.martin@mq.edu.au
[b] School of Chemistry, The Australian Centre for Nanomedicine and the ARC Centre of Excellence in Convergent Bio-Nano Science & Technology, University of New South Wales, Sydney, NSW 2052, Australia. E-mail: p.thordarson@unsw.edu.au

naphthalene-based capping group,[29–32] which has the advantages of not being base-labile and boasts several sites for additional functionalisation. Other popular capping groups which have previously been reviewed include the carboxybenzyl and cinnamoyl groups,[33–35] which due to their decreased aromaticity, require hydrophobic peptide sequences such as diphenylalanine to form hydrogels. The photoresponsive spiropyran, azobenzene and dansyl-based capping groups have also previously been reviewed.[36]

The alteration of the N-terminal capping group sits alongside other strategies such as selection of peptide sequence and gelation method in facilitating the tuning of peptide self-assembly and the properties of the resultant hierarchical structures. This review is not exhaustive but will selectively focus on recent progress made in expanding the chemical diversity of moieties which have been used to cap the N-terminus of short aromatic peptides. In addition to broadening the chemical landscape available to researchers, these new capping groups have yielded insights into the design rules which govern the self-assembly of short peptides into hydrogels, whilst concomitantly generating new functional materials.

Heterocyclic capping groups

Heterocycles are abundant in nature (*i.e.*, many drug molecules, the amino acid tryptophan, nucleic acids) and are a good starting point for expanding the chemical diversity of the N-terminal capping group in short peptides. As early as 2012, the capping of a pentapeptide Ala-Gly-Ala-Gly-Ala (AGAGA) sequence with an ex-tetrathiofulvalene (exTTF) was reported.[37] In this example, the TTF group is positioned either side of the 9- and 10-positions of an anthracene group, resulting in a deviation from planarity. This, associated with the hydrophobicity imparted by the anthracene group, yielded the formation of helical nanofibers where the TTF units do not interact with each other. These nanofibers formed only in halogenated organic solvents, with ageing behaviour (large bathochromic shifts in absorption spectra) observed in methylcyclohexane that could be reversed through the addition of methanol.

In 2014 Ulijn *et al.* attached a TTF group to a diphenylalanine peptide bearing an amine at its C-terminus (TTF-FF-NH_2, Fig. 1a) and observed gelation in several organic solvents including chloroform, ethyl acetate, DMSO and tetrahydrofuran.[38] Once gelation was established, the peptide was mixed with the acceptor tetracyano-*p*-quinodimethane (TCNQ) and iodine vapour to yield a supramolecular charge-transfer organogel, with characteristic peaks observed for $TCNQ^{\bullet -}$ and $TTF^{\bullet +}$ species. Drop casting of the organogel between gold contacts revealed a significant increase in conductivity upon incorporation of TCNQ, suggesting the successful generation of charge-transfer supramolecular nanofibers (Fig. 1b).

By switching from TTF group to naphthalene diimide (NDI), Ulijn *et al.* was able to form these charge-transfer supramolecular nanofibres in aqueous environments.[39] This was achieved through a biocatalytic pathway whereby the enzyme thermolysin was used to condense naphthalene diimide-tyrosine (NDI-Y) with phenylalanine amide (F-NH_2) in the presence of dialkoxynaphthalene derivatives, either 1,5-dialkoxynaphthalene (1,5-DAN) or 2,6-dialkoxynaphthalene (2,6-DAN). Upon the addition of the electron rich DAN donors, to the electron poor NDI-Y, a highly coloured charge-transfer complex was observed, corresponding to spherical aggregates. The addition of thermolysin induced the formation of a highly coloured hydrogel composed of charge-transfer nanofibres, which were imaged using AFM and charge-transfer confirmed using fluorescence spectroscopy.

Naphthalene diimides have also been used by Lin *et al.* to create multifunctional compounds which can be used for cell imaging or self-assemble into hydrogels at higher concentrations.

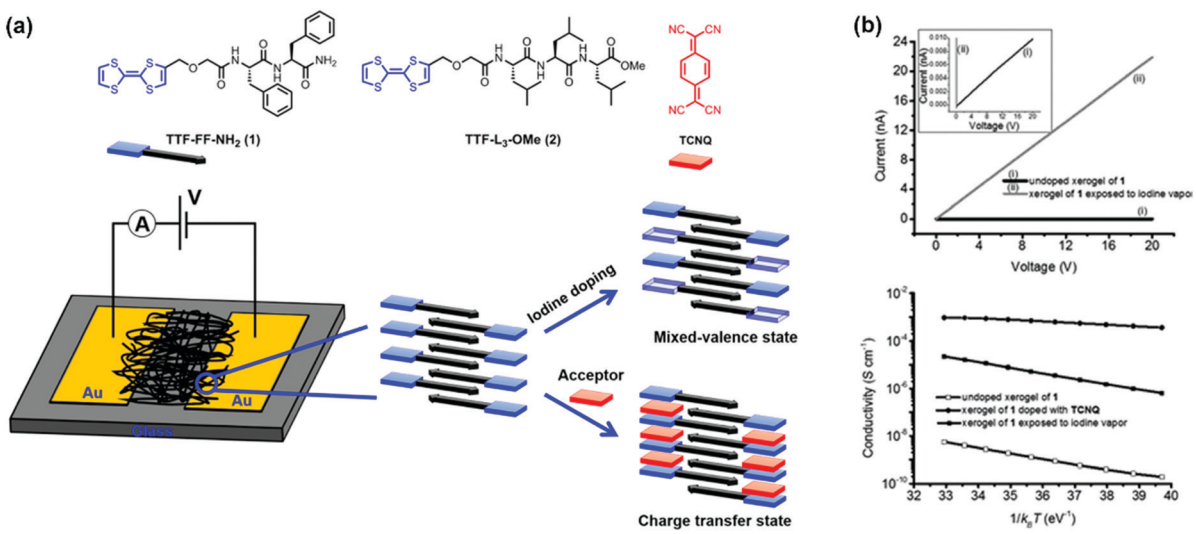

Fig. 1 (a) Schematic of conducting nanofibres composed of TTF-capped diphenylalanine and trileucine, doped with TCNQ as deposited across a gold electrode and their proposed self-assembly, (b) current–voltage (top) and conductivity (bottom) measurements showing significant enhancement upon exposure of TTF dried organogels to iodine vapour.[38] Copyright 2014, American Chemical Society.

Initially, a series of dipeptides composed of glycine/phenylalanine, capped at their N-terminus with a NDI group were synthesised (NDI-GG, NDI-GF, NDI-FG and NDI-FF).[40] All peptides were well tolerated by MCF-7 breast cancer cells, however, NDI-FG and ND-FF were found to be internalised and exhibited blue fluorescence. Interestingly, these two peptides were also the only ones able to form hydrogels at physiological pH, however, these studies were performed at far higher concentrations. NDI-based hydrogels were also obtained through mixing NDI-serine (NDI-S) and NDI-lysine (NDI-K) at neutral pH, with this co-assembly being the first example of an NDI-based hydrogel not bearing benzyl groups on the peptide side chain.[41] NDI-S and NDI-K were biocompatible up to 500 μM, but were only internalised into cells when mixed in a 1 : 1 ratio. The biocompatibility of this co-assembled peptide was not studied, however, it was shown that at higher concentrations (2% (w/v)), the 1 : 1 mixture of NDI-S and NDI-K gave hydrogels which had a stiffness of approximately 2 kPa.

In 2014, we reported the use of indole-3-acetic acid to cap to the N-terminus of diphenylalanine, giving indole-diphenylalanine (Ind-FF).[42] We theorised that the presence of the indolic hydrogen would allow for extensive hydrogen bonding between neighbouring peptides, resulting in a stiff hydrogel. This was indeed the case, with Ind-FF hydrogels displaying a storage modulus of 300 kPa, making them some of the stiffest peptide hydrogels reported. This high stiffness was due to the bundling of fibres in the hydrogel, whereupon individual 2 nm fibres associated together to give fibres hundreds of nanometers across, with hydrogel stiffness known to depend strongly on the degree of bundling.

Since our initial report, the indole capping group has been conjugated to the Gly-Phe-Phe-Tyr (GFFY) tetrapeptide *via* a propyl linker, forming hydrogels of moderate stiffness (~1 kPa) composed of 15–25 nm diameter fibres.[43] These hydrogels were then loaded with ovalbumin (10 wt% loading) and used as a vaccine adjuvant, with antibody production increased for hydrogel adjuvants compared to ovalbumin alone. Interestingly, slightly higher antibody production was observed for the Ind-GFFY composed entirely of D-amino acids, however, levels were still below the commercially available adjuvant Alum.

Following on from our work on the indole capping group, in 2015 we reported biocompatible scaffolds generated through the incorporation of a carbazole group at the N-terminus of either the dipeptide Phe-Phe (FF) or tripeptide Gly-Phe-Phe (GFF).[44] The carbazole group is structurally somewhat similar to the widely used Fmoc capping group, however, the absence of the carbamate linker means that it is stable towards basic conditions. Somewhat unsurprisingly given its structural similarity to Fmoc, carbazole capped diphenylalanine formed hydrogels with a very similar morphology to Fmoc-FF, featuring a highly branched network of nanofibers 2–3 nm in diameter (Fig. 2a). These peptides were shown to be supergelators (gelation observed at <0.05% (w/v)) and not cytotoxic towards HeLa cells at concentrations relevant to their self-assembly (Fig. 2b).

Shortly afterwards, Adams exploited the ability of carbazole to electropolymerise by synthesising carbazole-capped alanine (Carb-Ala).[45] Interestingly in this system, gelation could first be induced through a local pH change at the electrode surface (Fig. 2c) using a hydroquinone/quinone redox couple, before electrochemical polymerisation of the carbazole moieties to yield poly(Carb-Ala) films which could be reversibly switched between oxidised and reduced forms, offering control over hydrogel properties such as porosity.

We have described the ability of other heterocycles to promote gelation in diphenylalanine sequences, which have provided insight into developing structure–function relationships.[46] Benzimidazole-capped diphenylalanine was found to form hydrogels and single crystals (Fig. 3a).[47] This has been demonstrated previously for a number of peptide gelators including Fmoc and naphthalene-capped peptides,[48,49] however, this particular example is unique for the co-existence of nanocrystalline and fibrous domains as observed through atomic force microscopy (Fig. 3b). The crystal structure of this peptide suggested that at least in the solid state, the peptide adopts a parallel β-sheet conformation, contrary to current models of peptide self-assembly which suggest anti-parallel self-assembly.

Benzimidazolone-capped diphenylalanine has also been described, whereupon it was compared to several other peptide hydrogels and found to form branched hydrogels of moderate stiffness.[50] Phenothiazine (PTZ) has been used to cap the

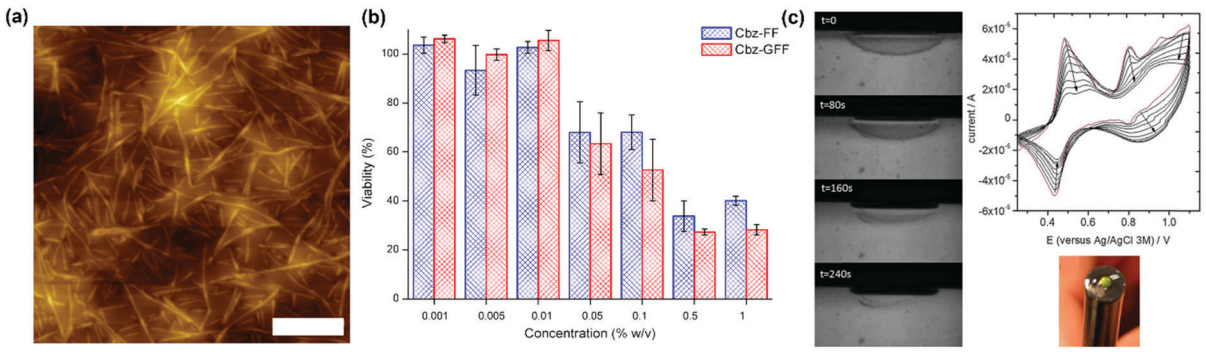

Fig. 2 (a) Atomic force micrograph of carbazole-diphenylalanine (Cbz-FF) showing uniform, 2 nm fibres, (b) solution cytotoxicity of Cbz-FF and Cbz-GFF towards HeLa cells after 24 h showing biocompatibility at low concentrations,[44] (c) *in situ* electrochemical polymerisation of carbazole-alanine (Carb-Ala) on the surface of a gold electrode over successive oxidation and reduction cycles.[45] Copyright 2015, Royal Society of Chemistry.

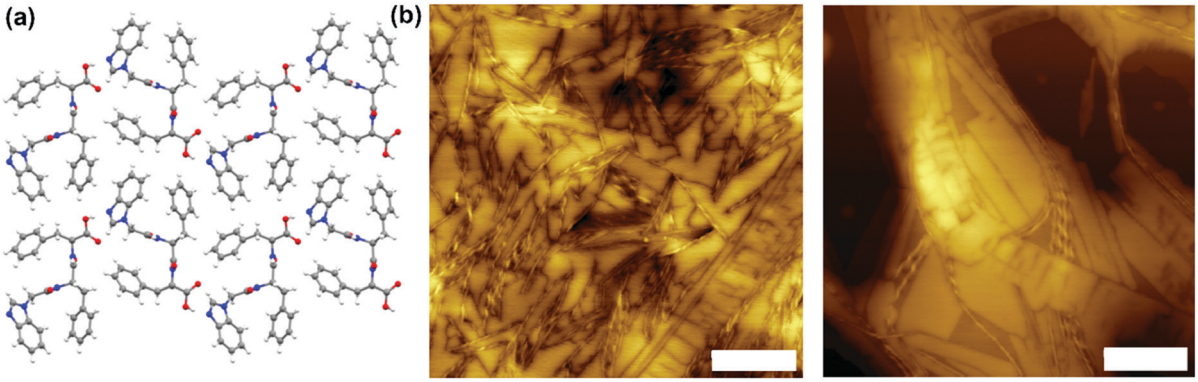

Fig. 3 (a) Crystal structure of benzimidazole-capped diphenylalanine and (b) atomic force micrographs showing simultaneous assembly into nanofibres and nanocrystals.[47] Scale bar represents 300 μm. Copyright 2016, American Chemical Society.

Gly-Phe-Phe (GFF) and Gly-Phe-Phe-Tyr (GFFY) peptide sequences.[51,52] As a 3D cell culture material, PTZ-GFF was shown to facilitate the growth of tumour spheroids, as opposed to Fmoc-GFF which showed cytotoxic effects. PTZ-GFF forms hydrogels at concentrations below 0.01% (w/v), with this low value attributed to the presence of a "pseudo-glycine" residue, identified through MM2 geometry optimisation calculations, due to the presence of the nitrogen at the 9-position of the heterocycle altering the conformation of the peptide, leading to more efficient stacking.

Fluorescent capping groups

Many of the aromatic moieties used to cap the N-terminus of short peptide hydrogels display some degree of fluorescence, due to the presence of aromatic conjugation. The well-studied Fmoc-group often exhibits fluorescence emission at approximately 310 nm, with a small shift associated with gelation.[53] For many of the aromatic capping groups used to cap short peptides, their fluorescence is quenched upon aggregation. Whilst this can be advantageous for tissue culture applications where minimisation of background fluorescence is desirable, an increase in fluorescence upon aggregation can yield fundamental insights into the self-assembly process. Peptides capped with the well-known aggregation-induced emitter (AIE) tetraphenylethylene (TPE) indeed show this type of behaviour. Liang *et al.* have reported examples of TPE attached to the N-terminus of the MAX1-derived MAX (KRKRGSVKVKVKV KDPPTVKVKVKVK-Am) and Q19 (KRKR-SGSG-QQEFQFQF KQQ-Am) peptides.[54,55]

The MAX peptide sequence was modelled on the well-established MAX1 peptide, however, introduced a KRKRGS spacer to increase water solubility and ensure no interference from the TPE group during the self-assembly process (Fig. 4a). The subsequent TPE-MAX peptide self-assembled into hydrogels as the pH was raised from 6.0 to 10.0. This resulted in a concomitant turn-on of fluorescence, where fluorescence intensity increased in a linear fashion from pH 8.7 to 9.9. Interestingly, fluorescence behaviour could be reversibly switched over multiple cycles by altering the pH between 6 and 10 (Fig. 4b), leading the authors to theorise that the system could be used as an intracellular pH sensor.

The same group also reported the conjugation of TPE to the Q19 peptide using a similar design strategy, where the resultant peptide formed a salt-responsive, fluorescent hydrogel (Fig. 4c). Fluorescence intensity was observed to increase proportionally to NaCl concentration, however, gelation only occurred at NaCl concentrations greater than 1 M. Fluorescence measurements at high dilution suggested that the AIE behaviour was due to the formation of nanostructures involving the TPE group, this was confirmed using circular dichroism.

TPE has also been used to cap the N-terminus of dipeptides, with TPE-GG, TPE-GF, TPE-FG and TPE-FF synthesised.[56] Out of these four peptides, only TPE-GG formed hydrogels at a concentration of 3% (w/v), the other peptides were found to be too hydrophobic. Microscopy studies revealed the formation of wide (300 nm) nanobelts. Fluorescence measurements of TPE-GG in DMSO:water mixtures of different volume fractions showed a 270× increase in fluorescence intensity when the water content increases from 80 to 99% (v/v), consistent with self-assembly of the peptide into nanostructures. Energy minimisation studies on a tetramer of TPE-GG suggested that a combination of amide-based hydrogen bonding and aromatic interactions between adjacent molecules are likely to cause suppression of rotational motion which results in a dramatic increase in fluorescence upon self-assembly.

Changing the linker from acetyl to oxyacetyl resulted in the ability to form hydrogels of TPE-FF through the addition of sodium chloride, with the gelation mediated through the addition of calcium chloride or glucono-delta-lactone (GdL) leading to syneresis,[57] which is when water is expelled from the hydrogel, typically due to network rearrangement. It was noted that no aggregation-induced emission was observed for gelation *via* sodium chloride or GdL, however, a large fluorescence increase was obtained over time when calcium chloride was used to trigger gelation. The authors ascribed this to a structural change which resulted in a more rigid packing arrangement for calcium triggered hydrogels, with these results offering insights into structural differences for hydrogels triggered using either a pH switch, monovalent or divalent cations.

Another example of an AIE-capped peptide was reported by Lin, who discovered the naphthaleneimide (NI) could be used

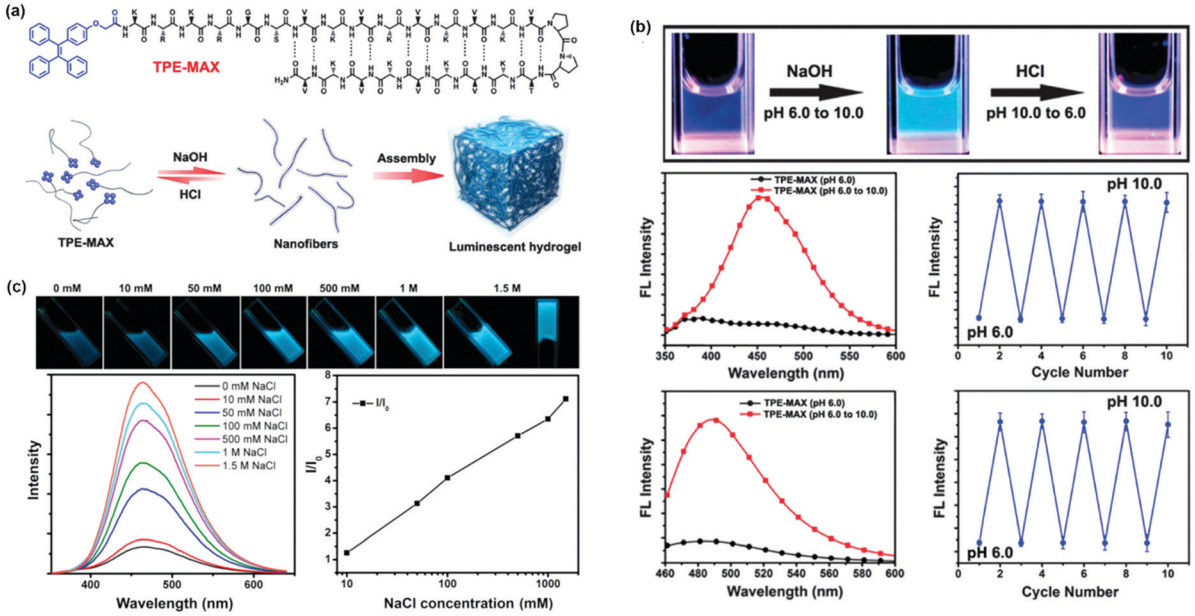

Fig. 4 (a) Design of tetraphenylethylene (TPE)-capped MAX peptide and subsequent self-assembly into luminescent hydrogels, (b) pH dependent fluorescence of TPE-MAX, showing switching of on and off fluorescent states across a number of pH cycles as measured by TPE-MAX fluorescence (middle) and Thioflavin T fluorescence (bottom).[54] Copyright 2014, American Chemical Society. (c) Salt-responsive fluorescence and gelation of the TPE-Q19 peptide.[55] Copyright 2015, Royal Society of Chemistry.

to cap the tripeptide sequence GFF to form fluorescent hydrogels at neutral pH.[58] Interestingly, when the reverse sequence FFG was used, under the same conditions no gelation was observed. In concentration dependent fluorescence measurements, the emergence of a new peak at 500 nm was observed for NI-GFF but not NI-FFG. As for the TPE gelators above, this was rationalised by the formation of emissive nanostructures, as evidenced through circular dichroism measurements and a ThT assay which suggested a secondary structure for NI-GFF but not NI-FFG peptides.

The attachment of a fluorophore to obtain resultant fluorescent hydrogel have also been reported. Wang *et al.* conjugated the fluorophore Rhodamine B to the peptide GFFY-CS-EE, where CS represents cysteine succinate and introduces a cleavable disulfide bond to the peptide (Fig. 5a).[59] Upon reduction with glutathione, the cleavage of the di-glutamic acid group reduces

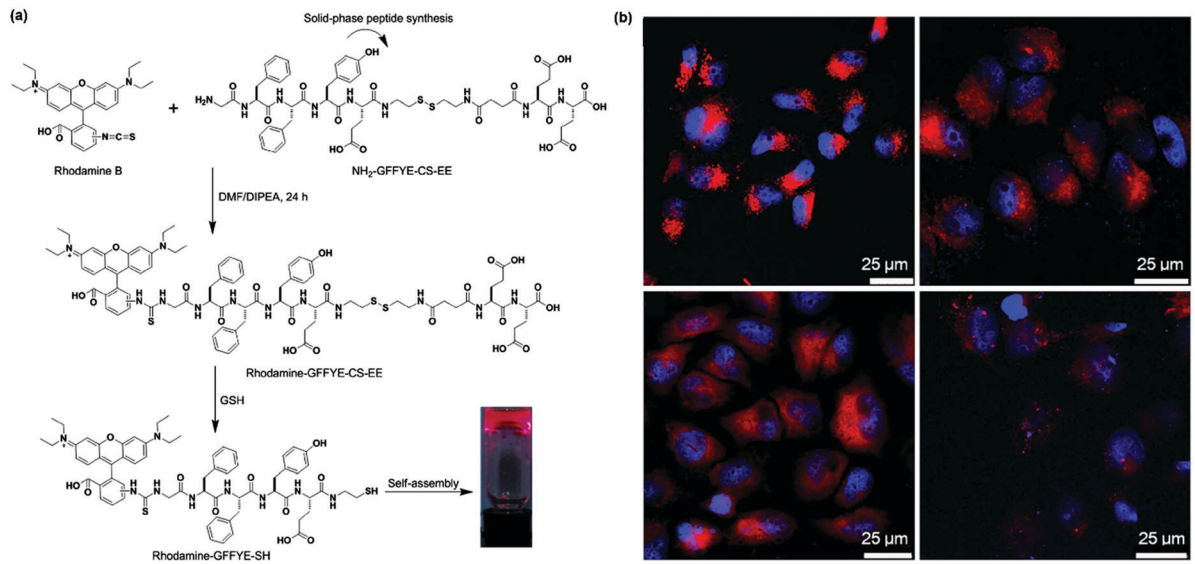

Fig. 5 (a) Synthesis of a rhodamine-capped pentapeptide and the subsequent formation of a fluorescent hydrogel through reduction with glutathione (GSH), (b) uptake and retention of rhodamine-GFFYE-SH peptides by HeLa cells for up to one (top left), three (top right), five (bottom left) and seven (bottom right) passages.[59] Copyright 2015, Nature Publishing Group.

the hydrophilicity of the peptide and results in self-assembly into a hydrogel. The hydrogel retains fluorescent properties and forms fibrous networks as observed through confocal and transmission electron microscopy. The hydrogel fibres were then diluted and successfully internalised into HeLa and HepG2 cells. An interesting application of this work was the use of the fluorescent nanofibers for cell tracking; it was shown that fluorescence was observed for up to 7 passages (Fig. 5b), compared to 3 passages for commercially available tracker CellTracker Green. This work demonstrates the promise of using fluorescent aggregates for cell tracking, however, it should be noted that no viability data was included. Furthermore, the authors described the accumulation of fluorescent nanofibres in tumours, likely due to the EPR effect.

In addition to Rhodamine B, fluorescein isothiocyanate (FITC) has been conjugated to the N-terminus of a short dileucine (-LL) peptide by Hamley *et al.*[60] FITC is widely used for labelling proteins and is known to react with free amines at or just above physiological pH. At low concentrations, FITC-LL was internalised by fibroblasts but was not cytotoxic, leading to potential applications as a cell staining reagent. Interestingly, it was shown that the dileucine peptide was required for internalisation, as FITC alone was not uptaken into cells. At higher concentrations, FITC-LL self-assembled into nanosheets which from small angle X-ray scattering studies were deemed to have a bilayer thickness of 8.9 Å, suggesting interdigitation of the peptides. It should be noted that at concentrations relevant to self-assembly, the fluorescence of the peptide was quenched.

Suzuki employed a custom cyanopyranyl fluorophore previously synthesised in-house and conjugated this to a peptide bearing two VEGF (Vascular Endothelial Growth Factor) binding sites, before immobilising the modified peptide onto magnetic beads.[61] It was found that the fluorescent capped peptide alone exhibited a strong fluorescent response upon introduction of VEGF, with a detection limit of 50 pg mL^{-1}, 500× lower than current commercially available kits. Specificity towards VEGF over albumin, lactic acid, creatine and placental growth factor were demonstrated, and upon immobilisation of the peptide sequence onto magnetic beads, the detection limit could be further lowered to 2 pg mL^{-1} after 1.5 h incubation time. Both this and the rhodamine B capped fluorescent hydrogels place emphasis on the requirement of a spacer between the fluorophore and the peptide, such that the presence of one group does not affect the functionality of the other.

The known fluorescent tag 4-nitro-2,1,3-benzoxadiazole (NBD) was used to cap the octapeptide Phe-Phe-Glu-Thr-Ile-Gly-Gly-Tyr (FFETIGGY) in order to form fluorescent nanofibres.[62] The peptide sequence was composed of the self-assembling diphenylalanine sequence at the N-terminus, followed by TIGGY, which is a sequence scramble of potassium binding peptides TXGYG, which are found in potassium channel. Importantly, as in previous examples, a two-carbon spacer was used such that fluorescence of the NBD group was retained. The NBD-capped octapeptide self-assembled into nanofibres in Tris–HCl solution with a low critical micelle concentration (0.14 mg mL^{-1}), whereas the octapeptide lacking the NBD group self-assembled, but did not form nanofibres. Four mammalian cells and two plant cells were treated with the fluorescent NBD-capped nanofibres, with internalisation observed for HeLa and Cos7 cells, but not for 3T3 and HepG2.

Wang *et al.* reported the generation of white-light emitting peptide hydrogels through the clever capping of the ionic complementary octapeptide sequence KFEFKFEF similar to those developed by Saiani,[63] with a tris(2,2′-bipyridine) (bipy) aromatic group (Fig. 6a).[64] This bipy-capped peptide formed hydrogels through mixing in phosphate buffered saline, with properties similar to the unmodified octapeptide, suggesting that the incorporation of the bipy group did not dramatically alter peptide self-assembly. It was theorised that the introduction of metal cations Eu^{3+}, Ir^{2+} and Ru^{2+} would cross-link the hydrogels due to the propensity of these metals to form octahedral tris(bipy) complexes. The addition of Eu^{3+} to the hydrogel resulted in a fluorescence turn-on (Fig. 6c), with neither the $EuCl_3$ nor octapeptide precursors displaying any fluorescent properties. The authors then tuned fluorescence emission through the incorporation of different metal Ir^{2+} and Ru^{2+}, giving yellow and red-emitting hydrogels, respectively, to complement the blue fluorescence of Eu^{3+} containing hydrogels (Fig. 6d). Through a trial-and-error method, the authors found that a ratio of Eu:Ir:Ru ratio of 20 : 1 : 0.5 resulted in white light emission under UV excitation, with Commission Internationale de L'Eclairage coordinates of (0.33, 0.33), suggesting potential applications in flexible light-emitting displays.

For fluorescently capped hydrogels to find uses in real-world applications such as sensing, biological and materials science, control over the photophysical behaviour of the materials in response to an applied stimulus is highly desirable. To this end, a number of photoresponsive peptide hydrogels have been reported. This review will not focus on photoresponsive and light-harvesting hydrogels, instead the reader is directed to excellent reviews on the topic by Adams and Gazit, respectively.[65,66]

Redox-responsive capping groups

One alternative to the use of fluorescent and light-responsive gelators are peptides which are redox-responsive. This is an especially relevant stimulus for cell-based work, where it is known that cancer and other diseased cells generate reactive oxygen species.[67,68] The Ulijn group has demonstrated several elegant examples of self-assembly catalysed through enzymatic and redox-responsive processes.[69–71] Similarly, many examples of peptide self-assembly upon reduction of a precursor (often containing a disulfide bond) using glutathione (GSH) exist in the literature.[72–76] This review, however, will focus on the imparting of redox-responsive behaviour to a peptide through its capping group.

Hydrogen peroxide is a commonly used reagent to demonstrate the utility of a redox-responsive material, as it is a simple small molecule with biological relevance. Hamachi *et al.* have described tripeptides based upon the diphenylalanine sequence and capped with a benzylic group substituted at the *para* position with a boronic acid (denoted BPmoc, Fig. 7a).[77] They note that

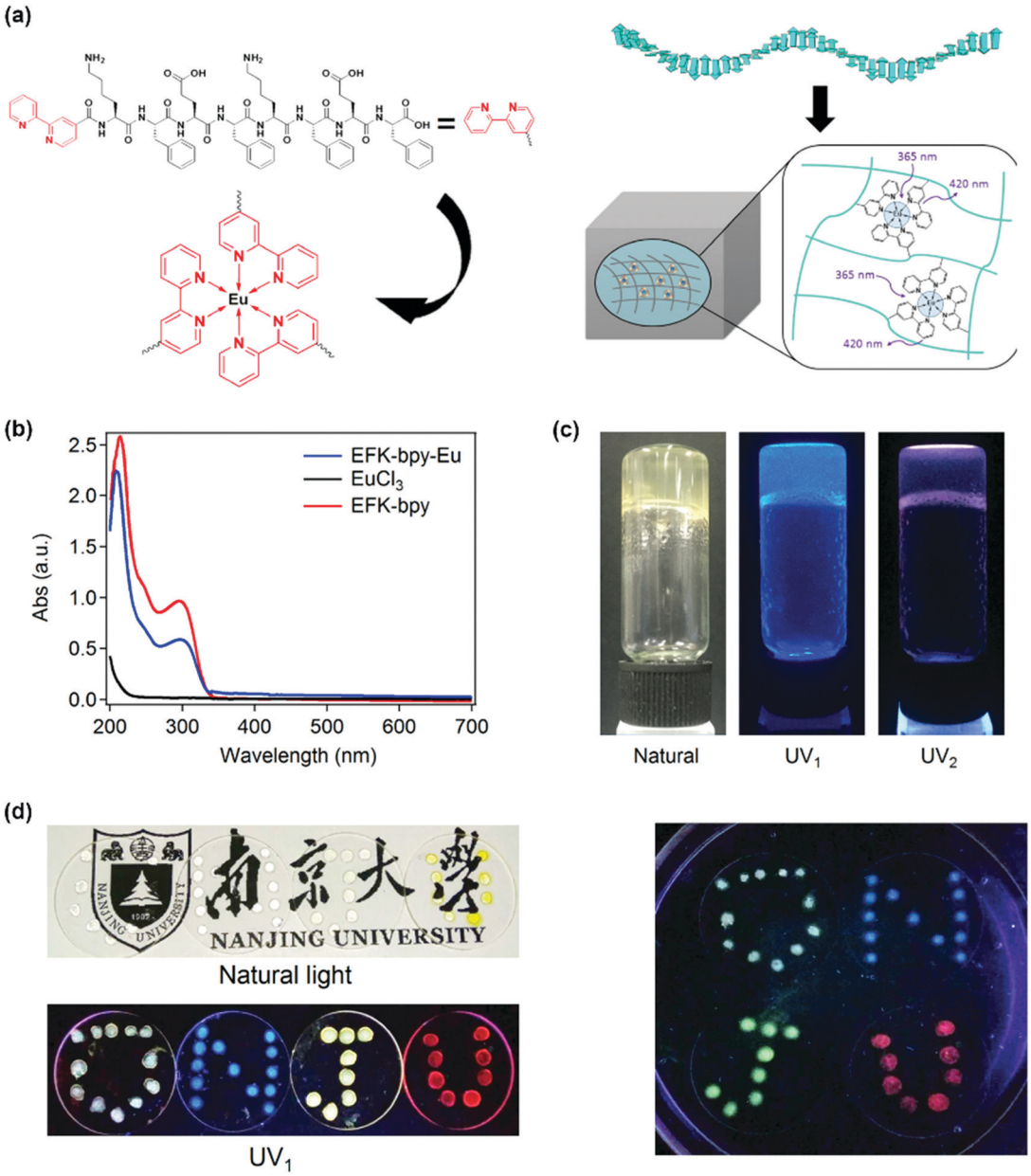

Fig. 6 (a) Synthesis of a complementary, ionic octapeptide capped with 2,2′-bipyridine and its cross-linking through addition of metal (in this case Eu^{3+}) cation. (b) Decrease in UV-Vis absorption upon metal incorporation, (c) but enhancement of fluorescence. (d) Creation of white-light emitting hydrogels through combination of Eu^{3+} (blue), Ir^{2+} (yellow) and Ru^{2+} (red) hydrogels and evaluation of their printability.[64] Copyright 2017, Nature Publishing Group.

BPmoc-capped peptides including BPmoc-FF, BPmoc-FFI, BPmoc-FFL and BPmoc-FFF all formed hydrogels, with BPmoc-FFF perhaps unsurprisingly having the lowest minimum gel concentration. Interestingly, out of the aforementioned gelators, BPmoc-FFF was found to be exceptionally sensitive to hydrogen peroxide, with only 0.5 molar equivalents required to facilitate complete collapse of the hydrogel network. Furthermore, it was established that only H_2O_2, and not O_2^- or OCl^-, resulted in hydrogel degradation, which was reported to occur at the carbamate bond. This phenomenon was exploited in encapsulating enzymes within BPmoc-FFF (Fig. 7b), where only the corresponding substrate yielded enzyme activity and the subsequent dissociation of the hydrogel (Fig. 7c). This was then extended to show sensitivity towards multi-step reactions, and ultimately multiple enzymes were encapsulated within the hydrogel as an example of a supramolecular logic gate.

The same group then used the peroxide-responsive BPmoc-FFF hydrogels to encapsulate an amplifier molecule in combination with sarcosine oxidase and urate oxidase for a visual detection assay as applied to uric acid levels in plasma.[78] In an elegant design strategy, the reaction of uric acid and urate oxidase results in peroxide generation, which then reacts with the amplifier molecule to produce two molecules of sarcosine, which subsequently reacts with the encapsulated sarcosine

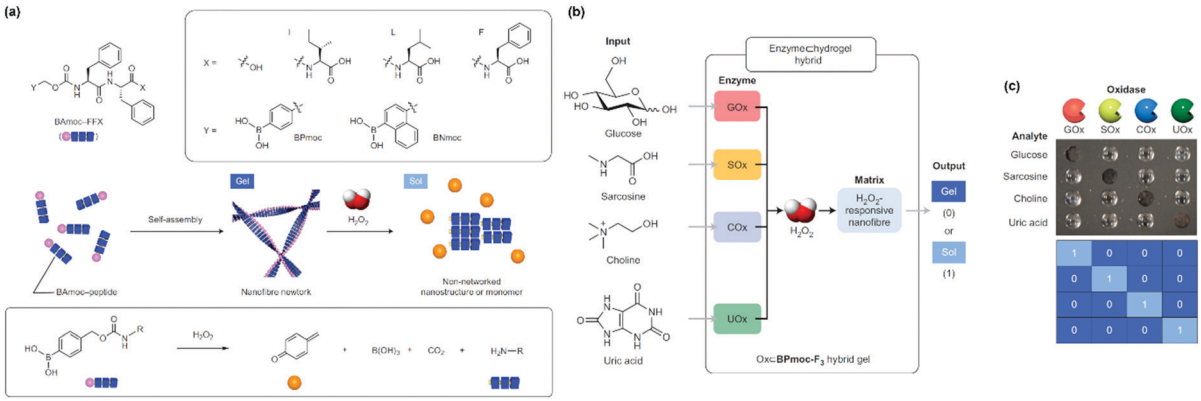

Fig. 7 (a) Synthesis, self-assembly and mechanism for peroxide-mediated disassembly for redox-responsive BPmoc-tripeptides, (b) their application in encapsulating enzymes, (c) inducing selective disassembly when exposed to the complementary substrate.[77] Copyright 2014, Nature Publishing Group.

oxidase to yield yet more peroxide molecules. This cascade of increasing peroxide generation then serves to disassemble the hydrogel, resulting in a visual detection method for the presence of uric acid. The authors showed that the encapsulation of enzymes and the signal amplifier did not affect the mechanical properties of the hydrogel. The utility of this method was demonstrated through substitution of urate oxidase with glucose oxidase, creating a glucose sensor with a threshold response of 0.10 mM.

A modified BPmoc capping group, NPmoc, where the boronic acid was replaced with a nitro group, was used to visualise the self-sorting of a two-component hydrogel.[79] Similarly to other studies, self-assembly (or disassembly) upon response to different stimuli is the key to successfully deconstructing this process. The NPmoc capping group is redox responsive, disassembling in the presence of the reductant sodium dithionite. When paired with the peptide amphiphile analogue Phos-cycC_6, which forms fibres that are reinforced through the addition of bacterial alkaline phosphatase, self-sorted hydrogels are obtained (Fig. 8a). In addition to visualising the self-sorting phenomenon, the redox-responsive nature of NPmoc was used to control the motion of encapsulated nanobeads (Fig. 8b). Here, the presence of the NPmoc group demonstrates that redox can be used as an orthogonal stimulus in multicomponent hydrogels.

Ferrocene is another well-studied, redox-responsive molecule. The attachment of the ferrocene (Fc) to self-assembling short peptides has been reported by Qi *et al.*[80] Here, ferrocene was either attached to the N-terminus of the diphenylalanine peptide. For Fc-FF, self-assembly upon dilution of a methanol solution into water resulted in the formation of nanospheres, which further aggregated into nanofibres upon external stimuli such as shaking or incubation at temperatures above 20 °C, suggesting a delicate equilibrium between spheres and fibres. Cyclic voltammetry (CV) was used to monitor this dynamic assembly process and revealed a reduction in peak current densities and shifting half wave potential upon a transition from nanospheres to nanofibres. The nanofibrous hydrogel could be disassembled through the addition of an oxidant, $CeSO_4$, which gave a CV profile consistent with the presence of monomeric species, and a concomitant change in appearance from a turbid yellow suspension to a transparent blue solution. The hydrogel could be recovered through the addition of reductant glutathione, however, only one cycle was presented.

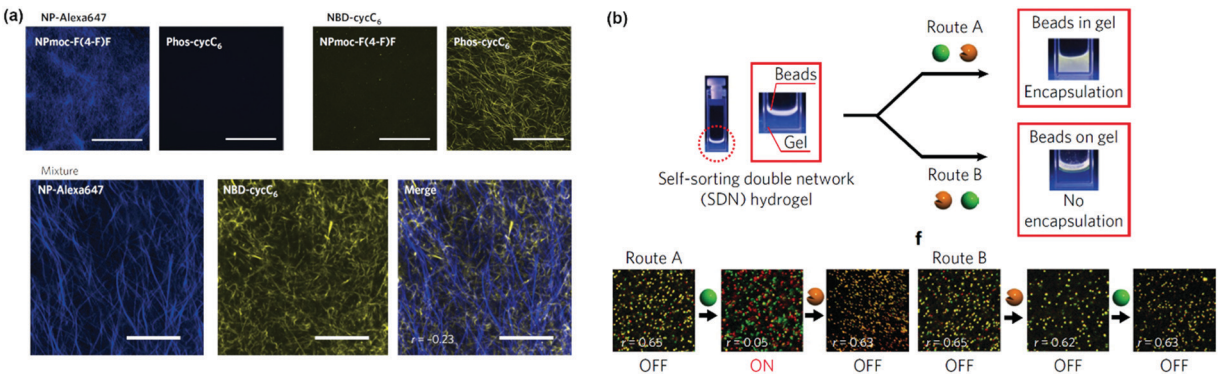

Fig. 8 (a) The visualisation of the self-sorting of redox-responsive NPmoc-F(4-F)F, labelled with an Alexa647 dye, and peptide amphiphile Phos-cycC_6 labelled with NBD (scale bar 50 μm). (b) Control of nanobead encapsulation through orthogonal stimuli, where the order of external stimulus application (sodium dithionite, green sphere or bacterial alkaline phosphatase, orange sphere) controls nanobead motion.[79] Copyright 2018, Nature Publishing Group.

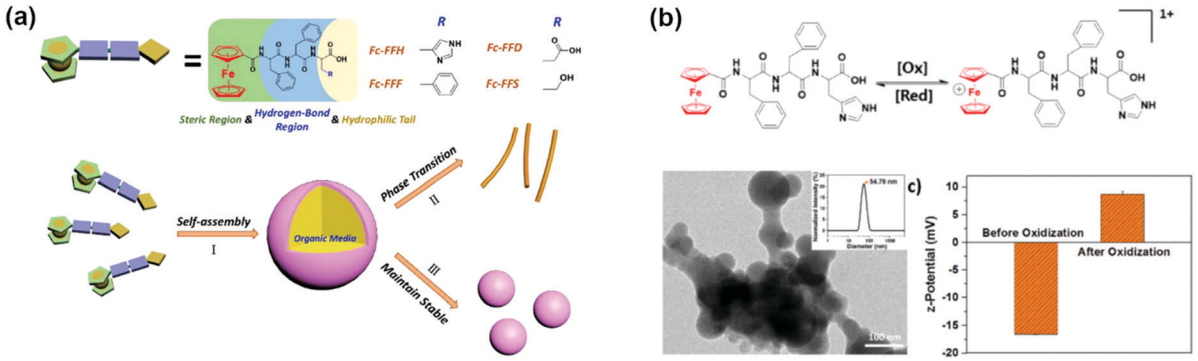

Fig. 9 (a) A series of ferrocene-capped tripeptides and their proposed selective self-assembly into nanofibres or nanospheres, (b) and transformation upon electrochemical oxidation to micellar aggregates.[81] Copyright 2017, Royal Society of Chemistry.

Ferrocene has also been attached to the tripeptides FFX, where X = histidine (H), phenylalanine (F), aspartic acid (D) or serine (S) (Fig. 9a).[81] These ferrocene-capped tripeptides were utilised to prepare nanoemulsions for phosphate buffer/ethyl acetate which were stable over the course of several months. Emulsions were not observed in the absence of the ferrocene group. The Fc-FFH peptide proved to be the most promising candidate for stabilising emulsions across a wide temperature range (20–70 °C), with hydrogels forming below 20 °C, which the authors propose is due to Ostwald's Rule of Stages. Electrochemical oxidation of the nanoemulsions yielded the formation of smaller, micellar aggregates (Fig. 9b), with the nanoemulsions unable to be recovered through electrochemical reduction.

Thus self-assembling peptides capped with redox-responsive group offer a promising method for controlling the assembly and disassembly of hydrogels. Electrochemical stimuli represent a controllable way to program assembly and disassembly, or morphological changes in supramolecular order, however, perhaps the most interesting applications of these materials lie within the biomedical field. It is known that the presence of disease alters the redox behaviour of the cell, and the use of small, self-assembling peptides in this context, either as a sensor or a delivery mechanism, has the potential to be highly beneficial.

Prodrug capping groups

One oft-cited possible biomedical application of self-assembling peptide hydrogels is drug delivery.[82,83] Here, a therapeutic is encapsulated within the hydrogel network and, constrained through pore size, diffusion-controlled release results in a more sustained dosage which is maintained within the therapeutic window, therefore reducing the number of doses required. Another possible way to achieve therapeutic, hydrogel-based delivery is to directly conjugate the drug molecule to the peptide. As the hydrogel is proteolytically degraded, the therapeutic is slowly released. This method has the advantage of circumventing problems associated with drug loading, however, the conjugation of a small molecule drug to a self-assembling peptide invariably alters its gelation ability, so care needs to be taken in the design step. It should be noted that an excellent review on self-assembling prodrugs by Cui exists, including some examples of self-assembling peptides capped with drug molecules.[84] For the sake of brevity, we will not discuss these examples in detail.

The Xu group has published a number of examples of prodrug-capped peptides. In 2013 they reported the use of NSAIDs naproxen, (*R*)-flurbiprofen, (*RS*)-flurbiprofen, (*RS*)-ibuprofen and aspirin as capping groups for dipeptides diphenylalanine (L and D enantiomers), FFY (again, L- and D-enantiomers) and dialanine.[85] Successful gelation was achieved for naproxen (dialanine, both enantiomers of FF and FFY), (*R*)-flurbiprofen (both FF enantiomers), (*RS*)-flurbiprofen (dialanine, L-FF) and (*RS*)-ibuprofen (L-FF) capping groups. Aspirin-capped peptides were unable to form hydrogels, presumably due to their lower hydrophobicity. For the majority of diphenylalanine hydrogels, a heat-cooling method was used to facilitate gelation, with a pH switch favoured to obtain dialanine hydrogels, and an enzymatic method applied to tyrosine-containing hydrogels. Whilst hydrogel characterisation was performed for all gelators, cytotoxicity investigations were only carried out on the naproxen-capped FF, FFY and FF(phos)Y where the hydroxyl group on the tyrosine is phosphonated. IC_{50} values of 206, 294 and 321 μm respectively were obtained, which is lower than the minimum gel concentration for each of the peptides. This suggests that the molecules are not well-suited to *in vitro* or *in vivo* applications.

To ameliorate the cytotoxicity of the above peptide hydrogels, likely due to the hydrophobicity associated with the diphenylalanine peptide and its ability to disrupt cellular membranes, Xu *et al.* then employed the diphenylalanine dilysine (FFKK) tetrapeptide sequence, capped at its N-terminus with racemic ibuprofen, indomethacin or (*S*)-(+)-naproxen (Fig. 10a).[86] Gelation for these peptides was achieved through acidification of a basic peptide solution and the resultant hydrogels fully characterised. The anti-microbial, anti-inflammatory and haemolytic activity of these NSAID-peptides were also evaluated (Fig. 10b–d). Naproxen-capped FFKK was shown to be the only of the three peptides which had bactericidal activity against all four bacteria selected, spanning Gram-positive and Gram-negative bacteria. Somewhat surprisingly, minimal concentration-dependent effects were observed for all peptides tested. Anti-inflammatory activity of the NSAID-peptides were assessed through a COX-2 inhibition

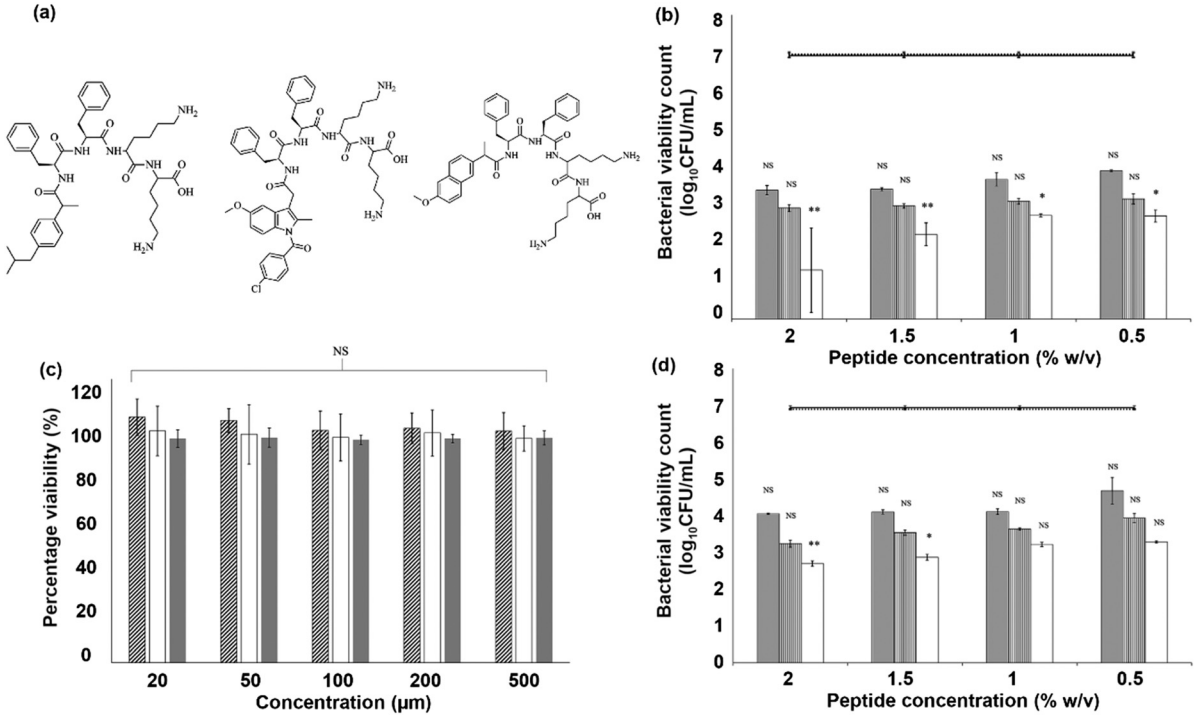

Fig. 10 (a) Structure of tetrapeptides FFKK capped with ibuprofen (left), indomethacin (middle and naproxen (right)), (b) their antibacterial activity against Gram-positive *S. aureus*, (c) evaluation of cytotoxicity against L929 fibroblasts and (d) antibacterial activity against Gram-negative *P. aeruginosa*.[86] Copyright 2016, Royal Society of Chemistry.

assay, with naproxen-capped FFKK again showing the most promising results. Lastly, none of the peptides exhibited significant haemolytic activity. The study shows that the interplay of both the NSAID and peptide sequence is important for retaining, and potentially improving, the efficacy of current NSAIDs.

Jana and Dastidar *et al.* also used the NSAID indomethacin as a capping group for peptides, namely the mono- and dipeptides phenylalanine, alanine, hydroxyproline, serine, threonine, hydroxyproline–serine, hydroxyproline–alanine, hydroxyproline–threonine and hydroxyproline–glycine.[87] Monopeptides capped with indomethacin were unable to form hydrogels, however, readily formed organogels in a number of solvents. All indomethacin-capped dipeptides, excepting hydroxyproline–alanine and hydroxyproline–glycine, formed hydrogels through a heat-cooling method in water, 0.9% (w/v) NaCl and PBS (pH 7.4). After studying the mechanical properties of the resultant hydrogels with rheology, indomethacin-capped hydroxyproline–threonine was the only NSAID-capped hydrogelator taken forward for biological testing. This dipeptide showed a cytotoxicity and anti-inflammatory profile similar to the parent indomethacin, however, these measurements were not undertaken in the gel phase.

Recently, Xu and Zhong *et al.* reported a clever dual delivery delivery strategy through immobilising the anti-cancer drug doxorubicin within a peptide hydrogel composed of indomethacin–Gly-Phe-Phe-Tyr-Arg-Gly-Asp-His, denoted IDM-GFFYGRGDH.[88] This motif incorporates both the GFFY self-assembly sequence which has been used previously,[52,59] an indomethacin capping group and the RGD cell adhesion moiety, which has high affinity for $\alpha_v\beta_3$ receptors overexpressed on tumour cells. Conjugation of doxorubicin was achieved through electrostatic interactions between the peptide and doxorubicin. Despite low levels of doxorubicin and indomethacin release being observed when the dox-loaded hydrogels were incubated in buffers designed to simulate the endosomal environment (8% release after 24 h), treatment of A549 cells with a combination of doxorubicin and the indomethacin peptide revealed decreased IC_{50} values compared to each individual treatment, suggesting a synergistic effect. It should however, be noted that the A549 cells were not treated with the compounds in the ''gel state'', although DLS measurements revealed a potential micellar arrangement of the peptide.

Yang *et al.* recently reported a number of NSAIDs used to cap the tetrapeptide sequence Gffy, where the lower case denotes the presence of D-amino acids (Fig. 11a).[89] Eight NSAIDs comprising flurbiprofen, carprofen, naproxen, ketoprofen, oxaprozin, fenoprofen, ibuprofen and fenbufen were conjugated to the Gffy tetrapeptide, with all peptides forming hydrogels in PBS. The immune adjuvant efficacy of these hydrogels was evaluated using ovalbumin as a model antigen (Fig. 11b), with flurbiprofen and carprofen-capped peptide hydrogels yielding the largest increase in OVA-antibody production. These two peptides, along with the naproxen-capped peptide hydrogel, were used in vaccinating C57BL/6J mice at 0 and 14 days, before an injection of tumour cells at day 21. All peptides inhibited tumourigenesis, with flurbiprofen and carprofen-capped peptides completely inhibiting any tumour growth whilst not affecting the viability of associated cells such as splenocytes

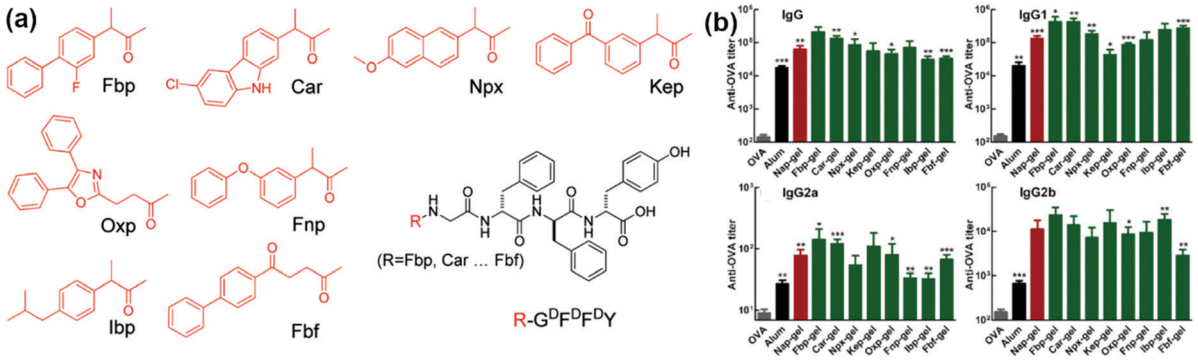

Fig. 11 (a) Eight NSAIDs used to cap the Gffy sequence and (b) the production of ovalbumin specific antibodies using these peptides as vaccine adjuvants, as quantified through mouse sera.[89] Copyright 2018, Royal Society of Chemistry.

and macrophages. Thus NSAID-capped peptides represent a promising approach to immunisation therapy.

Tumour suppression was also observed *in vivo* for BALB/c mice injected with 4T1 breast cancer cells and treated with oxaliplatin-capped peptides. In this study by Reithofer and Hauser *et al.*, the anti-cancer drug oxaliplatin was used to cap the peptides LIVAGK-NH_2, IVK-NH_2, LIVAGD-OH and IVD-OH through a click reaction.[90] Whilst the oxaliplatin-capped peptides were unable to gel, their acetylated precursors were, and upon mixing with oxaliplatin-capped peptides, a drug loading of 40 wt% could be achieved. The cytotoxicity of oxaliplatin-capped peptides was assessed using HeLa, SW480 and 4T1 cancer cell lines, with values in the low micromolar range observed. After confirmation of DNA platination and investigation of cell cycle arrest for all four oxaliplatin-peptide conjugates, *in vivo* administration of oxaliplatin-LIVAGK-NH_2, immobilised within a precursor hydrogel (Ac-LIVAGK-NH_2) showed tumour suppression, significant tumour accumulation and lower off-target cytotoxic side effects when compared to an oxaliplatin control.

Design of functional N-capped gelators

Although the introduction of specialised capping groups can impart functionality and responsiveness to self-assembling peptides, care must be taken when incorporating these groups onto the N-terminus of the peptide. Simply replacing an Fmoc group with a functional capping group of choice does not guarantee self-assembly.

A key consideration should be the hydrophobicity of the capping group to be used. The self-assembled state, among other things, is a balancing act between hydrophobic and hydrophilic interactions. The glycine-diphenylalanine sequence (-GFF) is an excellent example of this. We have previously shown that Fmoc-GFF forms self-supporting nanofibrous hydrogels which can be used as scaffolds for tumour spheroids.[51] Replacing the Fmoc with a phenothiazine,[51] or carbazole group[44] also yields hydrogels, however, when a less hydrophobic capping group is used, such as indole, benzimidazole or benzimidazolone, the peptide can no longer form hydrogels, nor even self-assemble.[91] Calculations of clog *P* show that the hydrogel-forming peptides above all have clog *P* values from 5.3–5.5, whereas the non-gelators have clog *P* values from 3–3.2.

The order of the peptide sequence used also plays a role, as all aforementioned capping groups self-assemble when attached to the ubiquitous diphenylalanine sequence. It has been reported that if a hydrophobic amino acid such as phenylalanine is positioned at the N-terminus of the peptide, that gelation is more likely.[92] This was observed for the naphthalene diimide peptides where NDI-FF and NDI-FG yielded hydrogels, but not NDI-GF or NDI-GG.[40] However, this is somewhat counteracted by the observation by Lin *et al.* where the tripeptide GFF capped with naphthaleneimide (NI-GFF) gave a fluorescent hydrogel, but no gelation was observed for NI-FFG.[58] It is known that even small perturbations in peptide sequence can have large effects on the behaviour of the resultant structures, this needs to be considered when designing new functional peptides.

When appending functional moieties onto the peptide N-terminus, the linker used to connect the capping group to the peptide sequence becomes very important, as it must not alter the functionality of the capping group, but it must also not interfere with self-assembly. This is dependent on the method of self-assembly, which is different for β-hairpin peptides like MAX1 and Q19 *versus* the diphenylalanine sequence.[93,94] This can be achieved through the introduction of alkyl linkers (although care must be taken to avoid excess flexibility which can be detrimental to gelation), the introduction of a peptide sequence spacer which is observed in the case of the aforementioned tetraphenylethylene (TPE) peptides,[54] or changing the chemistry from amides, to carbamates, to esters (Table 1).[95]

Conclusions

Significant progress has been made recently in incorporating different functional aromatic capping groups onto the N-terminus of peptides, ranging from commercially available fluorophores, to redox-responsive or electrochemically active molecules, to simple heterocycles, to synthetically complex prodrugs. The incorporation of functional aromatic capping groups onto the peptide N-terminus imparts properties which are not readily

Table 1 A list of capping groups described in this review, their chemical structures and applications

Structure	Name	Category	Applications	Ref.
	Tetrathiafulvalene	Heterocyclic	Supramolecular charge-transfer organogel	37 and 38
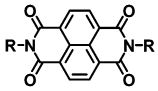	Naphthalene diimide	Heterocyclic	Supramolecular charge-transfer hydrogel, fluorescent cell tracking (MCF-7 cells)	39–41
	Indole	Heterocyclic	Scaffold for HeLa cells, vaccine adjuvant	42 and 43
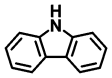	Carbazole	Heterocyclic	Scaffold for HeLa cells, electropolymer	44 and 45
	Benzimidazole	Heterocyclic	Insights into self-assembly, co-existence of crystal and gel phases	47
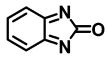	Benzimidazolone	Heterocyclic	Insights into self-assembly	50
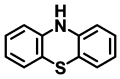	Phenothiazine	Heterocyclic	Permissive scaffold for tumour spheroids	51 and 52
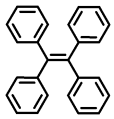	Tetraphenylethylene	Fluorescent	Aggregation-induced emitter, insights into self-assembly, potential pH sensor	54–57
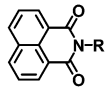	Naphthalene imide	Heterocyclic, fluorescent	Aggregation-induced emitter, insights into sequence dependent gelation	58
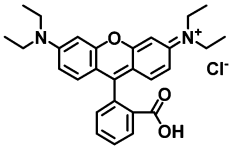	Rhodamine B	Fluorescent	Staining and tracking of HeLa and HepG2 cells for up to seven passages	59
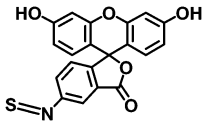	Fluorescein isothiocyanate	Fluorescent	Cell staining of human corneal fibroblasts	60
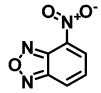	4-Nitro-2,1,3-benzoxadiazole (NBD)	Fluorescent	Cell uptake studies on four mammalian, two plant-based cell lines.	62
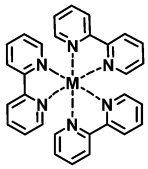	Metal complex with tris-2,2′-bipyridine	Heterocyclic, fluorescent	White light emitting material (through tuning metal cation)	64
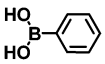	Phenylboronic acid (BPmoc)	Redox-responsive	Peroxide sensor, supramolecular logic gate, uric acid in plasma sensor	77 and 78
	Nitrobenzene (NPmoc)	Redox-responsive	Visualisation and selective disassembly of two-component hydrogel	79
	Ferrocene	Redox-responsive	Insights into self-assembly, stabilisation of emulsions	80 and 81
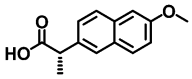	Naproxen	Prodrug	Slow release biomaterial (HeLa cells), antibacterial scaffold, tumour suppression	85, 86 and 89
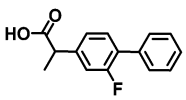	Flurbiprofen	Prodrug	Slow release biomaterial (HeLa cells), insights into self-assembly	85 and 89

Table 1 (*continued*)

Structure	Name	Category	Applications	Ref.
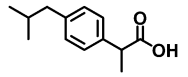	Ibuprofen	Prodrug	Slow release biomaterial (HeLa/L929 cells), potential antibacterial agent	85, 86 and 89
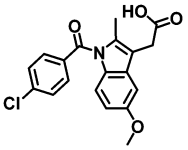	Indomethacin	Prodrug	Slow release biomaterial (RAW 264.7 macrophage), synergistic effect (with doxorubicin) on IC_{50} values against A549 lung cancer cells.	86–88
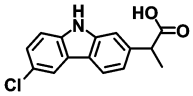	Carprofen	Prodrug	Vaccine adjuvant, tumour suppression	89
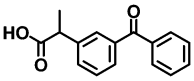	Ketoprofen	Prodrug	Vaccine adjuvant, tumour suppression	89
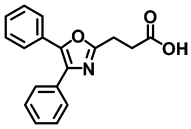	Oxaprozin	Prodrug	Vaccine adjuvant, tumour suppression	89
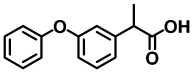	Fenoprofen	Prodrug	Vaccine adjuvant, tumour suppression	89
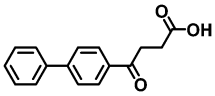	Fenbufen	Prodrug	Vaccine adjuvant, tumour suppression	89
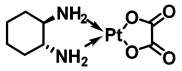	Oxaliplatin	Prodrug	Cytotoxicity evaluation (HeLa, SW480, 4T1), *in vivo* tumour suppression	90

accessible when using the ubiquitous Fmoc group. Through the incorporation of different functional capping groups, insights can be gained into the role of the N-terminus in peptide self-assembly, where design rules are still limited.

Looking forward, there are several areas where functional aromatic N-terminal capping groups will likely make an impact. Visualisation of the entire gelation process, from monomer to entangled network remains a challenge, however, significant progress has been made over the past decade, combining fluorescently labelled peptides with super-resolution optical microscopy. Intrinsically fluorescent N-terminal groups, or FRET pairs, may yield insights into this process. Improving optical microscopy capabilities, coupled with well-designed fluorescent peptides will also likely improve our understanding of the intracellular localisation of peptides, which will give insights into the route of internalisation and destination of different cell penetrating peptides, peptide-conjugated cargo or peptide-based scaffolds. With respect to peptide-based scaffolds for tissue engineering, little is known about which groups or ligands are presented at the nanofibre surface, and how this is affected by peptide sequence. This can be potentially be addressed through further incorporation of various capping groups, either ones with turn on/off fluorescence or chemically reactive modifications. Although most peptide-based sensors currently target extracellular processes, such as peroxide generation or glucose levels, the next frontier for these smart molecules must be intracellular sensing. The use of peptides in this scenario confers the potential of both targeting intracellular compartments and responsiveness to stimuli. Therefore, it is clear that the future is very promising for peptide-based materials, and that the modification of these peptides at their N-terminus with functional aromatic capping groups is an essential part of that toolbox.

Conflicts of interest

There are no conflicts to declare.

References

1 S. Sivakova and S. J. Rowan, *Chem. Soc. Rev.*, 2005, **34**, 9–21.
2 P. A. Gale, E. N. W. Howe and X. Wu, *Chem*, 2016, **1**, 351–422.
3 N. H. Evans and P. D. Beer, *Angew. Chem., Int. Ed.*, 2014, **53**, 11716–11754.
4 L. A. Churchfield and A. F. Tezcan, *Acc. Chem. Res.*, 2019, **52**, 345–355.
5 S. Bera, S. Mondal, S. Rencus-Lazar and E. Gazit, *Acc. Chem. Res.*, 2018, **51**, 2187–2197.
6 R. M. Nisbet, J. C. Polanco, L. M. Ittner and J. Goetz, *Acta Neuropathol.*, 2015, **129**, 207–220.

7 L. M. Ittner and J. Goetz, *Nat. Rev. Neurosci.*, 2011, **12**, 67–72.
8 B. Sun, K. Tao, Y. Jia, X. Yan, Q. Zou, E. Gazit and J. Li, *Chem. Soc. Rev.*, 2019, **48**, 4387–4400.
9 F. Ali, W. Raza, X. L. Li, H. Gul and K. H. Kim, *Nano Energy*, 2019, **57**, 879–902.
10 B. Apter, N. Lapshina, A. Handelman, B. D. Fainberg and G. Rosenman, *Small*, 2018, **14**, 1801147.
11 E. R. Draper and D. J. Adams, *Chem*, 2017, **3**, 390–410.
12 L. M. D. Rodriguez, Y. Hemar, J. Cornish and M. A. Brimble, *Chem. Soc. Rev.*, 2016, **45**, 4797–4824.
13 S. Marchesan, A. V. Vargiu and K. E. Styan, *Molecules*, 2015, **20**, 19775–19788.
14 E. R. Draper and D. J. Adams, *Chem. Soc. Rev.*, 2018, **47**, 3395–3405.
15 Z. Q. Q. Feng, T. F. Zhang, H. M. Wang and B. Xu, *Chem. Soc. Rev.*, 2017, **46**, 6470–6479.
16 M. Reches and E. Gazit, *Science*, 2003, **300**, 625–627.
17 L. Adler-Abramovich and E. Gazit, *Chem. Soc. Rev.*, 2014, **43**, 6881–6893.
18 K. Jenkins, S. Kelly, V. Nguyen, Y. Wu and R. S. Yang, *Nano Energy*, 2018, **51**, 317–323.
19 M. Reches and E. Gazit, *Isr. J. Chem.*, 2005, **45**, 363–371.
20 J. Raeburn, G. Pont, L. Chen, Y. Cesbron, R. Levy and D. J. Adams, *Soft Matter*, 2012, **8**, 1168–1174.
21 C. Tang, A. M. Smith, R. F. Collins, R. V. Ulijn and A. Saiani, *Langmuir*, 2009, **16**, 9447–9453.
22 D. J. Adams, M. F. Butler, W. J. Frith, M. Kirkland, L. Mullen and P. Sanderson, *Soft Matter*, 2009, **5**, 1856–1862.
23 V. Jayawarna, M. Ali, T. A. Jowitt, A. F. Miller, A. Saiani, J. E. Gough and R. V. Ulijn, *Adv. Mater.*, 2006, **18**, 611–614.
24 D. R. Nisbet, T. Y. Wang, K. F. Bruggeman, J. C. Niclis, F. A. Somaa, V. Penna, C. P. J. Hunt, Y. Wang, J. A. Kauhausen, R. J. Williams, L. H. Thompson and C. L. Parish, *Adv. Biosyst.*, 2018, **2**, 1800113.
25 D. Iglesias, M. Melle-Franco, M. Kurbasic, M. Melchionna, M. Abrami, M. Grassi, M. Prato and S. Marchesan, *ACS Nano*, 2018, **12**, 5530–5538.
26 C. Diaferia, M. Ghosh, T. Sibillano, E. Gallo, M. Stornaiuolo, C. Giannini, G. Morella, L. Adler-Abramovich and A. Accardo, *Soft Matter*, 2019, **15**, 487–496.
27 K. Tao, P. Makam and E. Gazit, *Science*, 2017, **358**, eaam9756.
28 W. T. Truong, Y. Su, D. Gloria, F. Braet and P. Thordarson, *Biomater. Sci.*, 2015, **3**, 298–307.
29 K. McAulay, B. Dietrich, H. Su, M. T. Scott, S. Rogers, Y. K. Al-Hilaly, H. Cui, L. C. Serpell, A. M. Seddon, E. R. Draper and D. J. Adams, *Chem. Sci.*, 2019, **10**, 7801–7806.
30 E. R. Draper, H. Su, C. Brasnett, R. J. Poole, S. Rogers, H. Cui, A. Seddon and D. J. Adams, *Angew. Chem., Int. Ed.*, 2017, **56**, 10467–10470.
31 E. R. Draper, E. G. B. Ebden, T. O. McDonald and D. J. Adams, *Nat. Chem.*, 2015, **7**, 848–852.
32 L. Chen, K. Morris, A. Laybourn, D. Elias, M. R. Hicks, A. Rodger, L. C. Serpell and D. J. Adams, *Langmuir*, 2009, **26**, 5232–5242.
33 D. M. Ryan, S. B. Anderson, F. T. Senguen, R. E. Youngman and B. L. Nilsson, *Soft Matter*, 2010, **6**, 475–479.
34 C. W. Ou, J. W. Zhang, X. L. Zhang, Z. M. Yang and M. S. Chen, *Chem. Commun.*, 2013, **49**, 1853–1855.
35 J. F. Shi, Y. A. Gao, Z. M. Yang and B. Xu, *Beilstein J. Org. Chem.*, 2011, **7**, 167–172.
36 G. Fichman and E. Gazit, *Acta Biomater.*, 2014, **10**, 1671–1682.
37 J. L. Lopez, C. Atienza, A. Insuasty, J. Lopez-Andarias, C. Romero-Nieto, D. M. Guldi and N. Martin, *Angew. Chem., Int. Ed.*, 2012, **51**, 3857–3861.
38 S. K. M. Nalluri, N. Shivarova, A. L. Kanibolotski, M. Zelzer, S. Gupta, P. W. J. M. Frederix, P. J. Skabara, H. Gleskova and R. V. Ulijn, *Langmuir*, 2014, **30**, 12429–12437.
39 S. K. M. Nalluri, C. Berdugo, N. Javid, P. W. J. M. Frederix and R. V. Ulijn, *Angew. Chem., Int. Ed.*, 2014, **53**, 5882–5887.
40 Y. H. Liu, S. M. Hsu, F. Y. Wu, H. Cheng, M. Y. Yeh and H. C. Lin, *Bioconjugate Chem.*, 2014, **25**, 1794–1800.
41 L. H. Hsu, S. M. Hsu, F. Y. Wu, Y. H. Liu, S. R. Nelli, M. Y. Yeh and H. C. Lin, *RSC Adv.*, 2015, **5**, 20410.
42 A. D. Martin, A. B. Robinson, A. F. Mason, J. P. Wojciechowski and P. Thordarson, *Chem. Commun.*, 2014, **50**, 15541–15544.
43 Z. Wang, Y. Cai, L. Yi, J. Gao and Z. Yang, *Chin. J. Chem.*, 2017, **35**, 1057–1062.
44 A. D. Martin, A. B. Robinson and P. Thordarson, *J. Mater. Chem. B*, 2015, **3**, 2277–2280.
45 P. S. Kubiak, S. Awhida, C. Hotchen, W. Deng, B. Alston, T. O. McDonald, D. J. Adams and P. J. Cameron, *Chem. Commun.*, 2015, **51**, 10427–10430.
46 A. D. Martin, J. P. Wojciechowski, A. B. Robinson, C. Heu, C. J. Garvey, J. Ratcliffe, L. J. Waddington, J. Gardiner and P. Thordarson, *Sci. Rep.*, 2017, **7**, 43947.
47 A. D. Martin, J. P. Wojciechowski, M. M. Bhadbhade and P. Thordarson, *Langmuir*, 2016, **32**, 2245–2250.
48 K. A. Houton, K. L. Morris, L. Chen, M. Schmidtmann, J. T. A. Jones, L. C. Serpell, G. O. Lloyd and D. J. Adams, *Langmuir*, 2012, **28**, 9797–9806.
49 J. Raeburn, C. Mendoza-Cuenca, B. N. Cattoz, M. A. Little, A. E. Terry, A. Z. Cardoso, P. C. Griffiths and D. J. Adams, *Soft Matter*, 2015, **11**, 927–935.
50 A. D. Martin, J. P. Wojciechowski, H. Warren, M. in het Panhuis and P. Thordarson, *Soft Matter*, 2016, **12**, 2700–2707.
51 J. P. Wojciechowski, A. D. Martin, A. F. Mason, C. M. Fife, S. M. Sagnella, M. Kavallaris and P. Thordarson, *ChemPlusChem*, 2017, **82**, 383–389.
52 C. Ou, J. Zhang, X. Zhang, Z. Yang and M. Chen, *Chem. Commun.*, 2013, **43**, 1853–1855.
53 K. Ryan, J. Beirne, G. Redmond, J. I. Kilpatrick, J. Guyonnet, N. V. Buchete, A. L. Kholkin and B. J. Rodriguez, *ACS Appl. Mater. Interfaces*, 2015, **7**, 12702–12707.
54 C. Zhang, C. Liu, X. Xue, X. Zhang, S. Huo, Y. Jiang, W. Q. Chen, G. Zou and X. J. Liang, *ACS Appl. Mater. Interfaces*, 2014, **6**, 757–762.
55 C. Zhang, Y. Li, X. Xue, P. Chu, C. Liu, K. Yang, Y. Jiang, W. Q. Chen, G. Zou and X. J. Liang, *Chem. Commun.*, 2015, **51**, 4168–4171.

56 M. Y. Yeh, C. W. Huang, J. W. Chang, Y. T. Huang, J. H. Lin, S. M. Hsu, S. C. Hung and H. C. Lin, *Soft Matter*, 2016, **12**, 6347–6351.
57 A. M. Castilla, B. Dietrich and D. J. Adams, *Gels*, 2018, **4**, 17.
58 M. Y. Yeh, C. T. Huang, T. S. Lai, F. Y. Chen, N. T. Chu, D. T. H. Tseng, S. C. Hung and H. C. Lin, *Langmuir*, 2016, **32**, 7630–7638.
59 H. Wang, D. Mao, Y. Wang, K. Wang, X. Yi, D. Kong, Z. Yang, Q. Liu and D. Ding, *Sci. Rep.*, 2015, **5**, 16680.
60 S. Kirkham, I. W. Hamley, A. M. Smith, R. M. Gouviea, C. J. Connon, M. Reza and J. Ruokolainen, *Colloids Surf., B*, 2016, **137**, 104–108.
61 Y. Suzuki, *Sens. Actuators, B*, 2018, **276**, 230–237.
62 J. Wang, J. Zheng, Y. Cai, J. Zheng, J. Gao, Q. Gong and Z. Yang, *Sci. China: Chem.*, 2016, **59**, 719–723.
63 A. Mujeeb, A. F. Miller, A. Saiani and J. E. Gough, *Acta Biomater.*, 2013, **9**, 4609–4617.
64 Y. Xia, B. Xue, M. Qin, Y. Cao, Y. Li and W. Wang, *Sci. Rep.*, 2017, **7**, 9691.
65 E. R. Draper and D. J. Adams, *Chem. Commun.*, 2016, **52**, 8196–8206.
66 P. Makam and E. Gazit, *Chem. Soc. Rev.*, 2018, **47**, 3406–3420.
67 A. Kaur, J. L. Kolanowski and E. J. New, *Angew. Chem., Int. Ed.*, 2016, **55**, 1602–1613.
68 D. Trachootham, J. Alexandre and P. Huang, *Nat. Rev. Drug Discovery*, 2009, **8**, 579–591.
69 J. K. Sahoo, C. G. Pappas, I. R. Sasselli, Y. M. Abul-Haija and R. V. Ulijn, *Angew. Chem., Int. Ed.*, 2017, **56**, 6828–6832.
70 A. Lampel, S. A. McPhee, H. A. Park, G. G. Scott, S. Humagain, D. R. Hekstra, B. Yoo, P. W. J. M. Frederix, T. D. Li, R. R. Abzalimov, S. G. Greenbaum, T. Tuttle, C. H. Hu, C. J. Bettinger and R. V. Ulijn, *Science*, 2017, **356**, 1064–1068.
71 C. Q. Shafi, R. Shafi, A. Lampel, D. MacPherson, C. G. Pappas, V. Narang, T. Wang, C. Maldarelli and R. V. Ulijn, *Angew. Chem., Int. Ed.*, 2017, **56**, 14511–14515.
72 Z. Zheng, P. Y. Chen, M. L. Xie, C. F. Wu, Y. F. Luo, W. T. Wang, J. Jiang and G. L. Liang, *J. Am. Chem. Soc.*, 2016, **138**, 11128–11131.
73 L. Lu, H. Liu, X. Chen and Z. Yang, *Colloids Surf., B*, 2013, **108**, 352–357.
74 Q. H. Xu, Z. Zhang, C. S. Xiao, C. L. He and X. S. Chen, *Biomacromolecules*, 2017, **18**, 1411–1418.
75 Y. Shi, J. Y. Wang, H. M. Wang, Y. H. Hu, X. M. Chen and Z. M. Yang, *PLoS One*, 2014, **9**, e106968.
76 H. K. Li, J. Gao, Y. Shang, Y. Q. Hua, M. Ye, Z. M. Yang, C. W. Ou and M. S. Chen, *ACS Appl. Mater. Interfaces*, 2018, **10**, 24459–24468.
77 M. Ikeda, T. Tanida, T. Yoshii, K. Kurotani, S. Onogi, K. Urayama and I. Hamachi, *Nat. Chem.*, 2014, **6**, 511–518.
78 T. Yoshii, S. Onogi, H. Shigemitsu and I. Hamachi, *J. Am. Chem. Soc.*, 2015, **137**, 3360–3365.
79 H. Shigemitsu, T. Fujisaku, W. Tanaka, R. Kubota, S. Minami, K. Urayama and I. Hamachi, *Nat. Nanotechnol.*, 2018, **13**, 165–172.
80 Y. Wang, R. Huang, W. Qi, Z. Wu, R. Su and Z. He, *Nanotechnology*, 2013, **24**, 465603.
81 X. Yang, Y. Wang, W. Qi, R. Su and Z. He, *Nanoscale*, 2017, **9**, 15323–15330.
82 K. Basu, A. Baral, S. Basak, A. Dehsorkhi, J. Nanda, D. Bhunia, S. Ghosh, V. Castalletto, I. W. Hamley and A. Banerjee, *Chem. Commun.*, 2016, **52**, 5045–5048.
83 J. Mayr, C. Saldias and D. Diaz Diaz, *Chem. Soc. Rev.*, 2018, **47**, 1484–1515.
84 A. G. Cheetham, R. W. Chakroun, W. Ma and H. Cui, *Chem. Soc. Rev.*, 2017, **46**, 6638–6663.
85 J. Li, Y. Kuang, J. Shi, Y. Gao, J. Zhou and B. Xu, *Beilstein J. Org. Chem.*, 2013, **9**, 908–917.
86 A. P. McCloskey, S. M. Gilmore, J. Zhou, E. R. Draper, S. Porter, B. F. Gilmore, B. Xu and G. Laverty, *RSC Adv.*, 2016, **6**, 114738–114749.
87 R. Roy, J. Deb, S. S. Jana and P. Dastidar, *Chem. – Asian J.*, 2014, **9**, 3196–3206.
88 L. Mei, S. he, K. Xu and W. Zhong, *Chem. Commun.*, 2019, **55**, 4411–4414.
89 Z. Wang, C. Lang, F. Shi, T. He, C. Gong, L. Wang and Z. Yang, *Nanoscale*, 2017, **9**, 14058–14064.
90 M. R. Reithofer, K. H. Chan, A. Lakshmanan, D. H. Lam, A. Mishra, B. Gopalan, M. Joshi, S. Wang and C. A. E. Hauser, *Chem. Sci.*, 2014, **5**, 625–630.
91 A. D. Martin, unpublished observations.
92 J. K. Sahoo, C. Nazareth, M. A. VandenBerg and M. J. Webber, *Soft Matter*, 2018, **14**, 9168–9174.
93 J. K. Kretsinger, L. A. Haines, B. Ozbas, D. J. Pochan and J. P. Schneider, *Biomaterials*, 2005, **26**, 5177–5186.
94 J. H. Collier and P. B. Messersmith, *Bioconjugate Chem.*, 2003, **14**, 748–755.
95 S. Fleming, S. Debnath, P. W. J. M. Frederix, T. Tuttle and R. V. Uijn, *Chem. Commun.*, 2013, **49**, 10587–10589.